OPTIMAL PERFORMANCE CHARACTERISTICS OF MORTAR INCORPORATING PHASE CHANGE MATERIALS AND SILICA FUME

Alan Richardson[1], Ashraf Heniegal[2], and Jess Tindall[3]

ABSTRACT

This paper examines the thermal performance of 20 different mortar mixes, which were prepared in order to study the behaviour of mortar incorporating Phase Change Materials (PCM). The PCM was used at a rate of 10, 20 and 30% by weight of total solid materials. Silica fume was added to the mixes by 10, 20, 30 and 50% by weight of cement to enhance the mortar properties. Mortars which incorporate phase-change materials (PCM) have the capability to help regulate the temperature inside buildings, contributing to the thermal comfort while decreasing the amount of mechanical heating and cooling energy required, therefore they have the potential to reduce building carbon emissions. The mechanical characteristics and physical properties of the mortar with PCM were studied. The results show that mortar with Phase Change Materials up to PCM20% can be used with an optimal compressive strength. Silica fume (SF), up to a 20% SF addition, enhanced the mechanical properties of the mortar.

KEYWORDS:

phase change material, mortar, silica fume, thermal conductivity

1. INTRODUCTION

Studies have been undertaken to investigate the potential benefit of incorporating PCM into various construction products. PCM can be used in solutions for walls, floors and ceilings either embedded with the plaster, plasterboard, render or placed in sealed packages above suspended ceilings. Their application takes advantage of the very significant amounts of thermal energy that these materials absorb as they melt and later release as they solidify. The melting, or transition, temperature is normally chosen to be approximately two degrees higher than the design air temperature of the room. As the space starts to become warmer than ideal (but not too hot) the PCM begins to melt and in doing so draws heat from the room thus helping the occupants remain more comfortable. Traditionally this goal has been achieved using concrete soffits to provide a high thermal mass, but PCM offers the potential to create a high thermal mass with similar benefits using much less material. There are several authors who have investigated

1 & 3. Department of Mechanical and Construction Engineering, Faculty of Engineering and Environment, Northumbria University, Tyne & Wear, UK NE1 8ST

2. Associate Professor, Department of Civil Constructions Department, Faculty of Industrial Education, Suez University, Egypt

constructive solutions, with the incorporation of PCM in floors. These solutions are varied, such as electric under floor heating systems incorporating polyethylene plates impregnated with PCM, incorporation of PCM in the concrete floor slab and the application of two types of PCM with different transition temperatures [1–4]. Silica fume (SF) is a very fine (typically less than one micrometre in diameter) industrial by-product used as a supplementary cementitious material to offer numerous benefits when included in concrete or mortar, including increased compressive and flexural strength (Siddique and Chahal 2011). SF used in combination with PCM can partially compensate for the reduction in these two physical parameters caused by adding PCM into the mortar mix.

This paper examines the incorporation of PCM in the construction process including the materials that constitute the fabric of buildings. PCM can be used in a range of structural components wherever swings in temperature need to be moderated, such as in the mortar to bed the brick or blockwork. However, PCM is most effective when used near the inner surface facing into the room, such as when mixed into a render or plaster. Siddique and Chahal [5] state that the addition of Silica Fume is beneficial in this application as it improves the mortars surface adhesion, however, care is needed as Appa Rao [6] confirms that a slight increase in the shrinkage rate is a consequence of adding SF.

Studies have been undertaken in order to investigate the thermal response of the building envelope to achieve a reduction in building energy demand. Internal temperature fluctuations can be minimised by designing high thermal mass into materials that constitute the building envelope [7–9]. Aste et al. 2009 [10] states that the implementation of walls with high thermal inertia reduces the energy requirements of heating and cooling systems, achieving a reduction of 10% in heating demand and 20% in cooling demand. This increase of the thermal mass can be enhanced by the addition of phase change materials (PCM). Izquierdo-Barrientos et al. [11] studied the optimal parameters to minimize the energy demand of a building due to heat transfer through the walls. They present a numerical simulation (6 days' winter and 6 days' summer) of a typical Spanish outer wall with a PCM layer where the orientation of the wall, the position of the PCM and the transition temperature were varied. The author concluded that the optimum transition temperature to minimise the thermal loads is dependent upon the orientation of the wall, the period of the year when the peak load reduction is desired and also the position of the PCM within the wall. Another study of building bricks containing PCM within their internal cylindrical holes has been carried out by Alawadhi et al. 2008 [12]. The results indicate a reduction of 17.5% of the heat flux at the indoor space when all three holes contain PCM and are placed at the centre line of the brick. Also, the proper location of the PCM inside the wall covered by a 12.7 mm gypsum wallboard, five foam insulating layers, and a 20.5 mm oriented strand board (OSB), has been evaluated using a dynamic wall simulator [13]. The results show an optimal location of 1/5L (L, is the width of the wall) from the internal surface of gypsum. The peak heat flux was reduced by 41% in this location, and the peak was shifted by approximately 2 hours. Furthermore, by using microencapsulated PCM the heat transfer area was increased, PCMs reactivity towards the exterior environment was reduced, and volume changes were controlled when the phase change occurs. The most common studies are carried out at a macro-scale, by numerical simulations, within a laboratory or at micro-scale to verify the improvement of microencapsulated PCM in the building envelope [14–19].

The thermal behaviour of PCM enhanced mortar is very important; however, the estimation of the mechanical properties is vital to facilitate the wider uptake of such mortars within

the construction industry. Data about the thermal and mechanical properties of mortars incorporating varying proportions of PCM with silica fume was one of the main gaps found within the published literature following an extensive literature review. Thus, the objective of this work was to design an experimental test programme to determine the physical and mechanical properties of mortars incorporating a range of combinations of PCM and silica fume and to identify optimal combinations to maximise the properties.

Twenty mortars, based on different PCM and silica fume percentages, were designed and prepared for laboratory testing. The following physical and mechanical properties were evaluated: bulk density, solid density, water absorption, pore volume, thermal conductivity, microstructure, compressive strength, flexural strength and tensile strength.

2. METHODOLOGY

The experimental test program was planned to achieve the research objective of this study as outlined in Section 1. The experimental work consisted of 20 mixes (comprised of 4 groups) of different mortars and each batch contained PCM incorporated at 0, 10, 20 and 30%. The PCM was batched by replacement of the total solids of the mix with each percentage of PCM, and each group contained 5 mixes with different SF% additions of 0, 10, 20, 30 and 50%. The control standard mortar (C100-SF0-PCM0) incorporated no PCM or silica fume. The fresh mortar of all mixes was mixed to the same consistency (measured with a flow test) using a superplasticizer addition for each group. In this research, two phases were studied, and these were the physical properties (bulk density, water absorption, voids volume, thermal characteristics and microstructures) and the mechanical properties (compressive, flexural and indirect tensile strength).

2.1 Specimens

The specimens used in this research were standard prisms of mortar (40x40x160 mm) and were batched in the laboratories at Northumbria University in accordance to the British Standard EN 1015-11:1999 [20] for both the compressive and flexural strength tests. Additionally, cubes of dimensions 100x100x100 mm were prepared for the indirect tensile strength test.

2.2 Materials and batching

The aggregate size used within this test programme was not greater than 2 mm for batching purposes and the test procedures employed were in accordance with BS EN 1015-1:1999 [21] and BS EN 1015-2:1999 [22]. The binder was composed of Portland cement 52.5N CEM I, to BS EN 197.1:2011 [23] and Elkem Microsilica grade 940 was used at varying percentage additions. Table 1 displays the chemical and physical properties of the composition of Elkem Microsilica. To minimise the water content (W) Sika ViscoCrete 35RM high-performance superplasticizer (SP) was used at 0.6–1.5% by weight of cement).

The Phase Change Material PCM used in this research was Microencapsulated phase change material (MPCM 24-D). This PCM is supplied as very small bi-component particles, powder like in appearance with a mean size of 17–20 microns, consisting of PCM as the core material encapsulated in a polymer outer shell. PCMs have melt points (transition temperatures) in the range of –30°C to 55°C, and these can absorb and release large amounts of heat during the phase change process. Table 2 shows the properties of MPCM 24-D.

TABLE 1. Chemical and Physical Properties of the Elkem Microsillica (Silica fume).

Property	Specifications (Characteristic values)
SiO_2 (%)	>90
H_2O (moisture content when packed, %)	<1
Loss in Ignition, LOI(%)	<3
Retained on 45 micron sieve (tested on undensified, %)	<1.5
Bulk density-undensified (when packed, kg/m^3)	200–350
Bulk density-densified (when packed, kg/m^3)	500–700

TABLE 2. MPCM 24-D product general properties.

Typical Properties	Specifications (Characteristic values)
Appearance W	White to slightly off-white colour
Form	Dry powder
Capsule Composition	85–90% wt.% PCM 10–15 wt.% polymer shell
Core Material	Paraffin
Particle size (mean)	17–20 micron
Melting Point	24°C (75°F)
Heat of Fusion	154–164 J/g
Specific Gravity	0.9
Temperature Stability	Extremely stable—less than 1% leakage when heated to 250°C
Thermal Cycling	Multiple

Table 3 shows the mix proportions of the mortar by weight and how the different samples are referenced to clearly display the mix proportions, simply from the mix ID.

TABLE 3. Mix Proportions of mortars.

Mix number:	Mix ID:	Cement-C (kg)	Sand (kg)	Silica fume-SF (kg)	PCM (kg)	SP/(C+SF+PCM)%	W/(C+SF+PCM)
1	C100-SF0-PCM0	1.00	3.0	0.00	0.0	0.00	0.45
2	C100-SF10-PCM0	0.90	3.0	0.10	0.0	2.15	0.45
3	C100-SF20-PCM0	0.80	3.0	0.20	0.0	2.50	0.45
4	C100-SF30-PCM0	0.70	3.0	0.30	0.0	2.70	0.45
5	C100-SF50-PCM0	0.50	3.0	0.50	0.0	2.90	0.45
6	C100-SF0-PCM10	0.90	2.7	0.00	0.4	1.92	0.45
7	C90-SF10-PCM10	0.81	2.7	0.09	0.4	2.72	0.45
8	C80-SF20-PCM10	0.72	2.7	0.18	0.4	2.92	0.45
9	C70-SF30-PCM10	0.63	2.7	0.27	0.4	3.50	0.45
10	C50-SF50-PCM10	0.45	2.7	0.45	0.4	4.19	0.55
11	C100-SF0-PCM20	0.80	2.4	0.00	0.8	2.36	0.50
12	C90-SF10-PCM20	0.72	2.4	0.08	0.8	2.85	0.50
13	C80-SF20-PCM20	0.64	2.4	0.16	0.8	3.08	0.50
14	C70-SF30-PCM20	0.56	2.4	0.24	0.8	3.72	0.50
15	C50-SF50-PCM20	0.40	2.4	0.40	0.8	4.00	0.50
16	C100-SF0-PCM30	0.70	2.1	0.00	1.2	2.45	0.69
17	C90-SF10-PCM30	0.63	2.1	0.07	1.2	3.10	0.69
18	C80-SF20-PCM30	0.56	2.1	0.14	1.2	3.25	0.69
19	C70-SF30-PCM30	0.49	2.1	0.21	1.2	3.88	0.69
20	C50-SF50-PCM30	0.35	2.1	0.35	1.2	4.30	0.69

The mortar mixtures were cast into standard moulds (40x40x160 mm) made of polystyrene with lids and 100 mm cubic polystyrene moulds (for testing indirect tensile strength) and all were manually compacted. The surfaces of the samples were covered with a low-density polyethylene cover over the polystyrene set moulds (3 specimens in each set) to prevent water evaporation during the initial curing. All specimens were stripped from the moulds after 24 hours and cured in water at 20°C for 28 days.

2.3 Thermal conductivity

A steady-state heat transfer test, illustrated in Figure 1 and based on the unguarded hot plate method, was used to calculate the thermal conductivity of the mortar samples.

FIGURE 1. Diagram of the thermal conductivity apparatus.

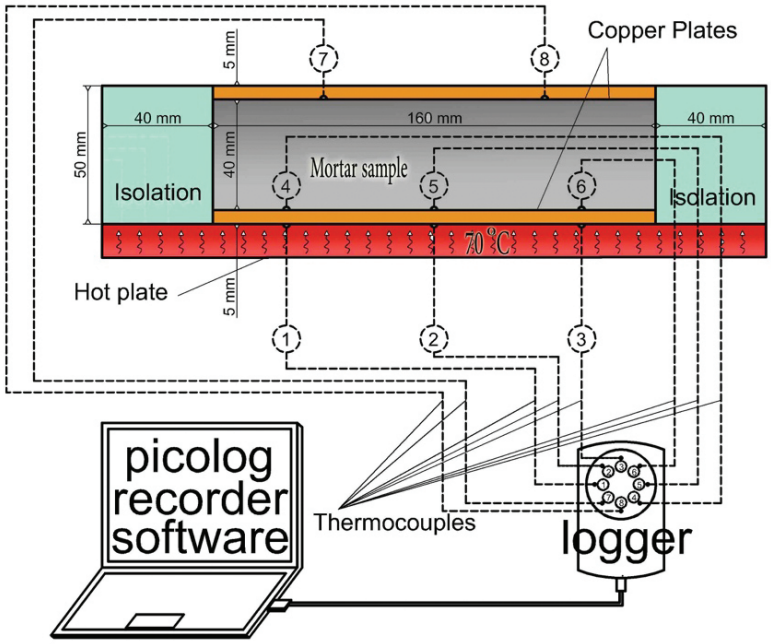

The copper plate was used to calibrate the thermocouples as part of the thermal conductivity measuring apparatus before measuring the thermal conductivity of mortar specimens. The test rig was arranged in a vertical alignment with a block of solid copper (5mm thickness with three thermocouples attached to the top and bottom surfaces) was placed on top of the hot plate, the test specimen and another copper block (with two thermocouples attached to the bottom surface). The hot plate was adjusted to 70°C. The mortar specimens were inserted between the two copper plates as shown in Figure 1. The three thermocouples connected under the bottom copper plate recorded the temperature of the hot plate. The three connected on the top surface of the bottom copper plate recorded the temperature at the interface of the copper plate and the bottom surface of the mortar sample. The two thermocouples connected to the underside of the top copper plate recorded the temperature at the interface of the mortar sample and bottom of the upper copper plate. Average temperatures were recorded for three measurement positions:

1. The underside of the bottom copper plate
2. The top side of the bottom copper plate and the underside of the mortar sample
3. The underside of the top copper plate and the upper surface of the mortar sample

The test rig was encapsulated within an insulating thermoplastic to minimise heat loss from the sides of the sample. All eight thermocouples were connected to a software program (Picolog Recorder) which in turn was connected to the laptop for recording the temperature at the eight points as shown in Figure 1. Specimens were tested for approximately 5 hours or until there was no more than a 0.2°C temperature change over a 15 minute period.

The known thermal conductivity of the copper plate permitted the calculation of the rate of heat transfer through it and therefore also through the mortar sample, (Q) as Equation [1]

$$Q = (k_c) \cdot (A_c) \cdot (\Delta T_c)/(\Delta X_c) \text{ for copper} \qquad [1]$$

Where, (A_c) is the area (m^2) of copper plate; (ΔX_c), the thickness (m) of copper plate; (Q) the heat transfer (W) through copper plate; (ΔT_c) the temperature difference (°C) of the copper plate; and (k_c) the thermal conductivity (W/mK) of copper plate. Using the average temperatures recorded at steady state conditions for both sides of the mortar sample, the thermal conductivity of the mortar sample can be calculated as shown in Equation [2]:

$$k_m = (Q_c \cdot \Delta X_m)/(A_m \cdot \Delta T_m) \quad [2]$$

Where, (A_m) is the area (m^2) of mortar; (ΔX_m), the thickness (m) of mortar; (Q_c) the heat transfer (W) through the copper plate (and also through the mortar sample) as indicated in Equation 1; (ΔT_m) the temperature difference (°C) across the mortar; and (k_m) the thermal conductivity (W/mK) of mortar.

2.4 Pore volume

The calculation of pore volume was achieved by fully saturating the test specimens in a curing tank [24]. Richardson et. al [25] determined specimens to be fully saturated after 72 hours or when the specimen weight changes less than 1 percent by bulk density in a 24-hour period. The sample weight is recorded when fully saturated, at the surface dried state, then specimens are oven dried at 110°C until the weight change is less than 1 percent of bulk density. The weight of each oven dried specimen was recorded, and Equation 3 applied to determine the pore volume percentage of the specimens:

$$P_v = \rho_w (m_s - m_o)/V \quad [3]$$

where ρ_w is the density of water (0.998g/cm^3) at 21°C; m_s the mass of saturated specimen (g); m_o the mass of oven dried specimen (g); P_v the pore volume (percent); and V the volume of the specimen (cm^3).

2.5 Indirect tensile strength (Brazilian test—ASTM D3967-08)

The Brazilian test is identified as a split-tensile test for the tensile strength of concrete. The Brazilian test is conducted under compression, and thus the fracture process might be different from that in the direct tension test. There is no standard test procedure for the tensile strength of mortar. However, there is a common method for calculating tensile strength through indirect tensile tests. A splitting test can be carried out on a standard cylinder or prism specimen by applying a line load along the vertical diameter. In this test, 100x100x100 mm cubes were used for the indirect test (Brazilian test). A steel rod 10 mm diameter was centred over a layer of wood strip as indicated in Figure 2 as a line load of the cube surface. The indirect tensile strength was calculated according to the Equation [4]:

$$ITS = 2P/(\pi \cdot DL) \quad [4]$$

Where:

ITS, indirect tensile strength (MPa)

P, applied load (kN)

D, diameter of the inside circle tangent of the square of the cube (m)

L, length of line load (m)

FIGURE 2. Indirect tensile test (Brazilian test).

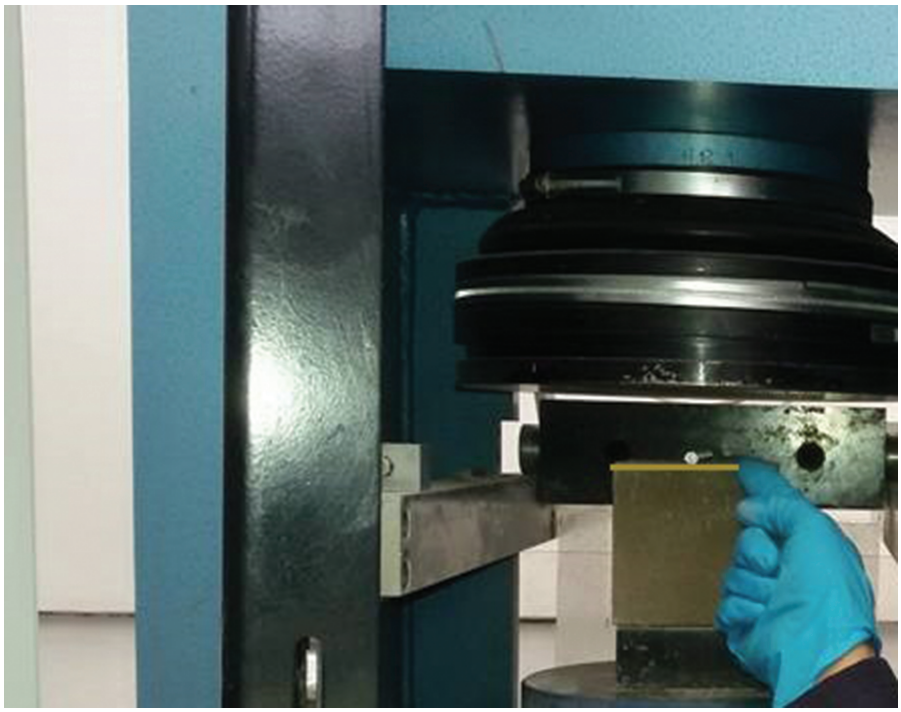

3. RESULTS AND DISCUSSION

3.1 Physical properties of PCM mortar

Bulk density, density, pore volume percentage, absorption percentage, thermal conductivity and microstructure using a Scanning Electron Microscope (SEM) were studied in this research. Table 4 displays the properties of the mortars.

3.1.1 Bulk density

Bulk density was determined using the standard dry method [26]. The results indicate that all bulk densities decreased when the PCM % increased for all samples. The bulk density of specimens without silica fume were reduced to 88.5, 70.7 and 66.9% relative to the control specimens C100-SF0-PCM0. The use of silica fume decreases the bulk density of mortars containing PCM by a small value as shown in Figure 3 and Table 4, using SF10%, the relative bulk densities were 87.4, 70.1 and 63.6% where these values with SF50% were 83.1, 65.6 58.9%. It is noted that both PCM and silica fume display a reduction of the bulk density of the mortars.

3.1.2 Density

All specimens were tested by using samples placed on a scaled water container and measuring the increase in water height which represents the volume of mortar solids only without any voids or moistures. The density was determined by dividing the sum of the weight of each ingredient (kg) by the volume of the mortar without pores.

TABLE 4. Properties of mortars

Mix NO:	Mix ID:	Compressive strength MPa		Flexural strength MPa	Indirect splitting strength MPa	Bulk density (kg/m^3)	Solid density (kg/m^3)	Void volume%	Thermal conductivity W/mK
		7 days	28 days						
1	C100-SF0-PCM0	20.95	28.52	3.50	2.65	1807	1888	9.30	1.25
2	C100-SF10-PCM0	22.80	34.52	3.60	2.7	1790	1862	9.67	1.22
3	C100-SF20-PCM0	23.42	36.20	3.42	2.9	1768	1855	10.05	1.18
4	C100-SF30-PCM0	21.88	33.45	3.15	2.76	1750	1822	10.41	1.11
5	C100-SF50-PCM0	17.22	23.78	2.75	2.42	1712	1800	10.77	1.05
6	C100-SF0-PCM10	12.75	18.21	2.93	1.89	1599	1705	18.10	1.08
7	C90-SF10-PCM10	14.32	20.10	3.00	1.98	1580	1680	18.55	0.95
8	C80-SF20-PCM10	15.12	20.87	2.75	2.15	1566	1650	19.22	0.91
9	C70-SF30-PCM10	13.52	19.65	2.62	2.04	1533	1630	20.19	0.87
10	C50-SF50-PCM10	11.03	16.00	2.37	1.66	1501	1550	21.10	0.83
11	C100-SF0-PCM20	7.63	11.56	2.40	1.22	1277	1363	26.00	0.86
12	C90-SF10-PCM20	9.78	14.03	2.55	1.32	1266	1321	26.75	0.81
13	C80-SF20-PCM20	10.63	14.61	2.32	1.52	1236	1289	28.10	0.77
14	C70-SF30-PCM20	9.10	12.89	2.20	1.42	1219	1260	29.78	0.74
15	C50-SF50-PCM20	6.02	9.50	1.93	1.00	1185	1250	31.48	0.70
16	C100-SF0-PCM30	3.76	4.30	1.66	0.75	1209	1297	33.00	0.75
17	C90-SF10-PCM30	5.50	6.55	1.75	0.86	1150	1240	33.85	0.72
18	C80-SF20-PCM30	6.63	6.20	1.65	1.05	1120	1200	34.42	0.68
19	C70-SF30-PCM30	5.02	5.50	1.55	0.92	1100	1148	35.00	0.63
20	C50-SF50-PCM30	2.56	3.90	1.43	0.35	1064	1100	36.20	0.60

FIGURE 3. Bulk density of mortars incorporating PCM.

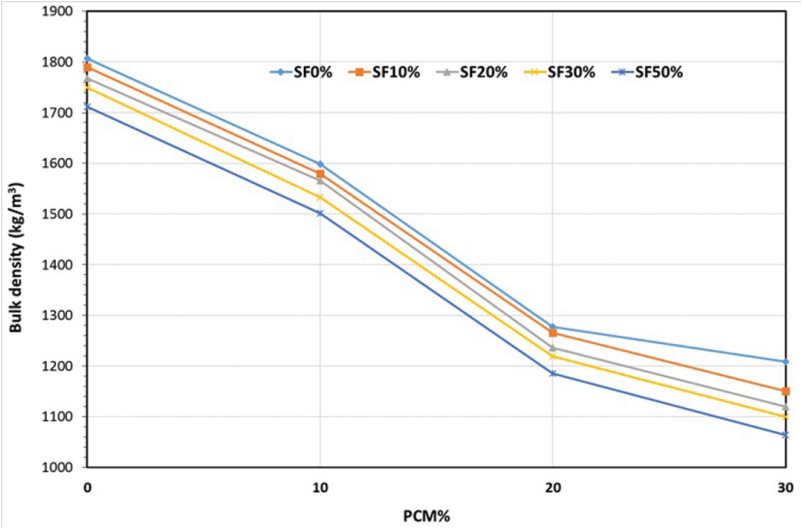

FIGURE 4. Density of mortars incorporating PCM.

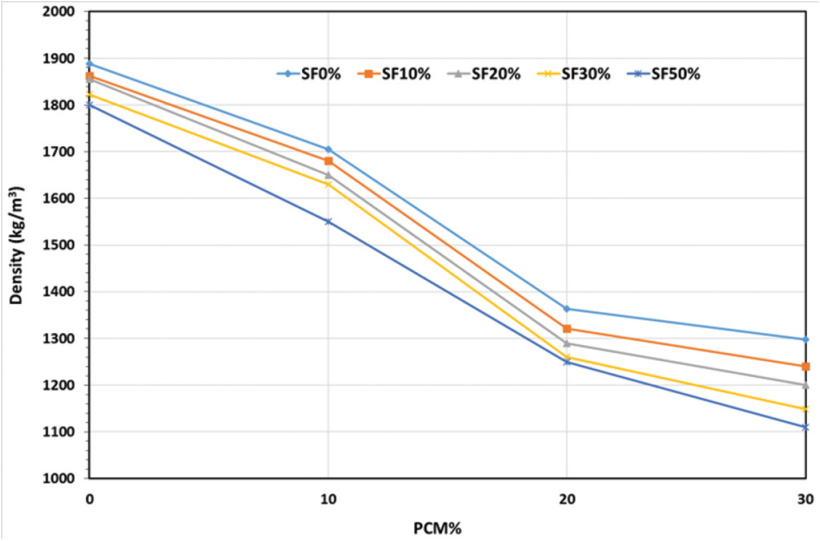

The results indicate that PCM in mortar decreases the density. For specimens that do not contain silica fume, the density decreased with PCM% compared to the control mix C100-SF0-PCM0; where it decreased to 90.3, 72.2 and 68,7% for 10, 20 and 30% PCM respectively as represented in Figure 2 and Table 4. The effect of the silica fume decreases the density for all percentages of PCM where these values were 89.0, 70.0 and 65.7% for SF10% and 82.1, 66.2 and 58.3% for SF50% respectively.

3.1.3 Water absorption

Water absorption of mixes containing PCM increased with an increasing PCM% as shown in Figure 5 and Table 4. This correlates with the results of both bulk density and density where pores increase inside the mortars that include PCM; hence water absorption increases for all specimens.

FIGURE 5. Water absorption of mortars incorporating PCM.

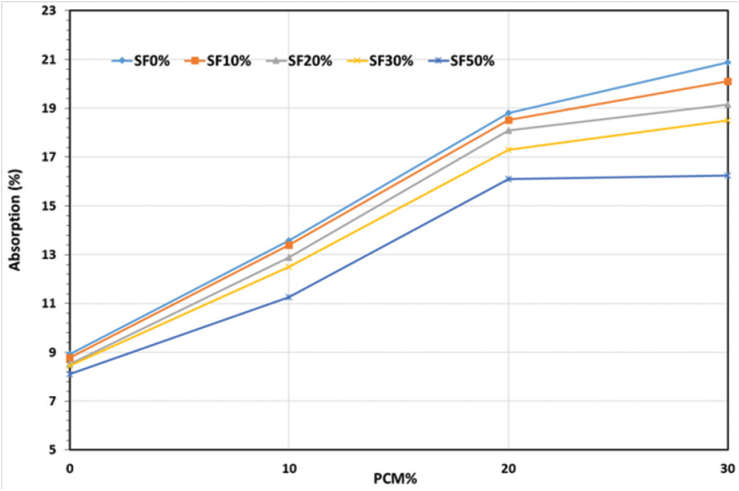

For samples without silica fume, the water absorption was 9.92% for the control mix, and this increased gradually with PCM content until it recorded 20.89% for PCM30%. In addition, silica fume slightly decreases the water absorption as follows: 20.10% for SF10% and 16.25% for SF50% and PCM30%.

3.1.4 Pore volume %

Pore volume % were recorded for all specimens and the results in Table 4 and Figure 6 report that pore volume % increases with PCM%. The pore volume % was 9.3% for the control mix and increased up to 33.0% for PCM30% for the specimens without silica fume. However, silica fume decreased the pore volume of the specimens where it reached to 36.2% for SF50% and PCM 30%.

FIGURE 6. Pore volume % for mortar incorporating PCM.

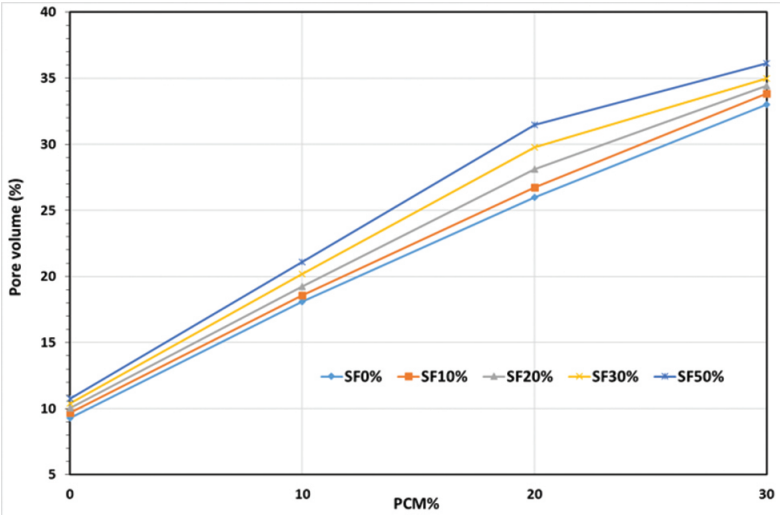

Results of both pore volume percentage and water absorption were recorded. Figure 7 presents the data with regard to the effect of pore volume on the water absorption of the mortar.

FIGURE 7. Relation between pore volume % and Water absorption% of mortars incorporating PCM.

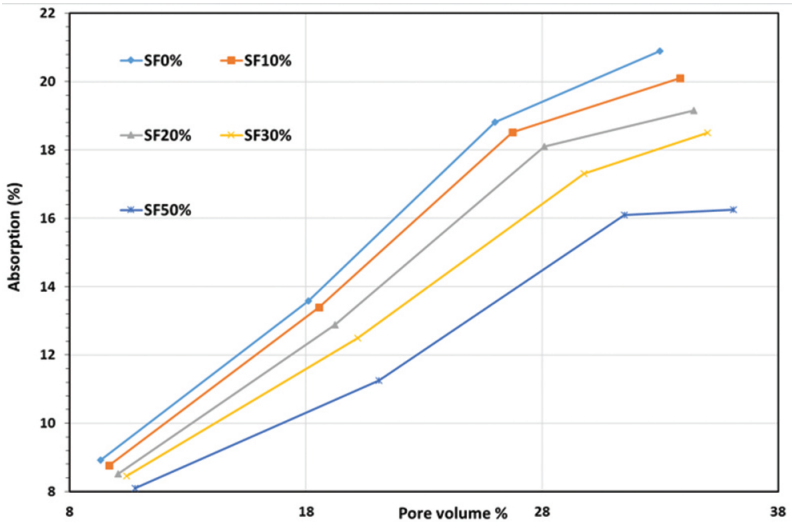

3.1.5 Thermal properties

3.1.5.1 Thermal conductivity

The results of the thermal conductivity are displayed in Figure 8. It can be seen that the heat transfer of the mortar specimens incorporating PCM decreases compared to the control mixes thermal conductivity which was 1,25 W/mK.

FIGURE 8. Thermal conductivity of mortar incorporating PCM.

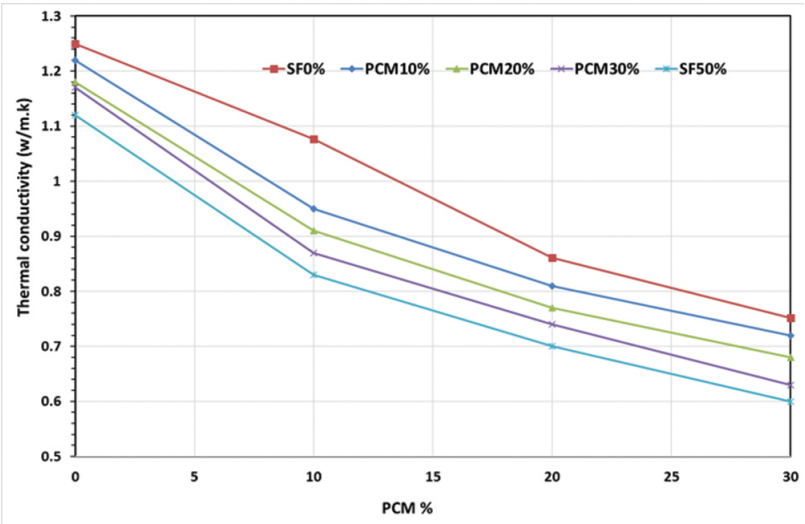

This value was reduced to 0.6 W/mK using PCM30% and SF50%. The relative thermal conductivity percentage of all specimens with different amounts of PCM compared to the control mortar are displayed in Figure 9 which shows that the thermal conductivity of the mortar was reduced for all samples when compared to the control mix. Results indicate that the specimens without silica fume which contained 10, 20 and 30% PCM exhibited relative

thermal conductivities of 86.4, 68.8 and 60.0% respectively in comparison to the control mix which was considered to be 100%. Using silica fume also reduced these values of relative thermal conductivities proportionate to the SF%. Adding SF10% to the mortar containing PCM 10, 20 and 30%, gives relative thermal conductivities of 76.0, 64.8 and 57.6% respectively in comparison to the control mix. Adding SF50% to the mortar containing PCM 10, 20 and 30% gives relative thermal conductivities of 66.4, 56.0 and 48.0% in comparison to the control mix.

Equation [2] can be used to estimate the Thermal Conductivity of a mortar mix incorporating PCM with SF to within ±2% for SF10 through SF30 and ±10% for SF0 and SF50.

$$k_{\text{m-PCM}} = -0.000015 \cdot PCM\%^3 + 0.0011 \cdot PCM\%^2 - 0.0362 \cdot PCM\% + k_{\text{m}} \cdot (-0.0035.SF\% + 1.01)$$

Where; ($k_{\text{m-PCM}}$) is the Thermal Conductivity of the mortar incorporating PCM and SF (W/m^{2}K); ($PCM\%$) is the percentage of PCM incorporated into the mortar; (k_{m}) is the Thermal Conductivity of standard mortar (W/m^{2}K); ($SF\%$) is the percentage of SF.

FIGURE 9. Relative thermal conductivity (%) of mortar incorporating PCM compared to the control mortar.

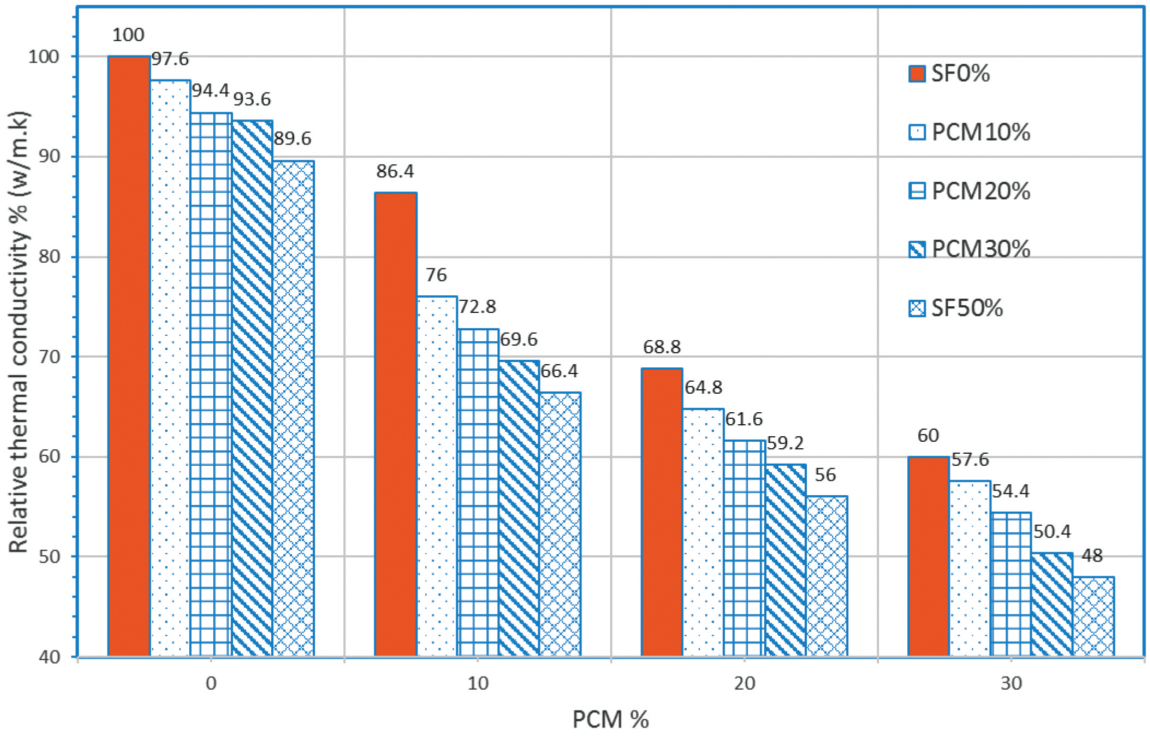

3.1.6 Scanning Electron Microscope Results

Polished surfaces of all specimen were examined in a scanning electron microscope (SEM, MIRA3 TESCAN 70µm, Northumbria University, Newcastle, UK). The results are displayed in Figures 10, 11 and 12.

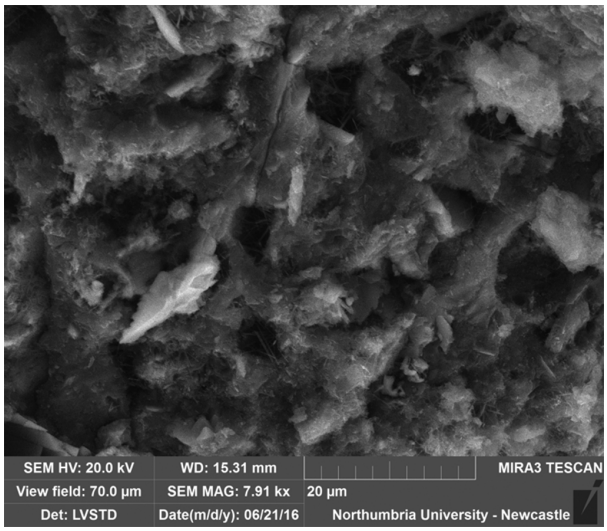

FIGURE 10. Control mortar (C100-SF0-PCM0).

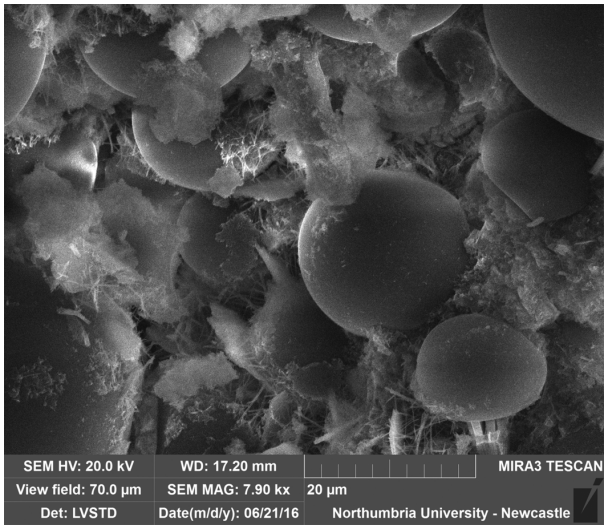

FIGURE 11. Mortar with PCM20% and no SF (C100-SF0-PCM20)—broken particle ringed.

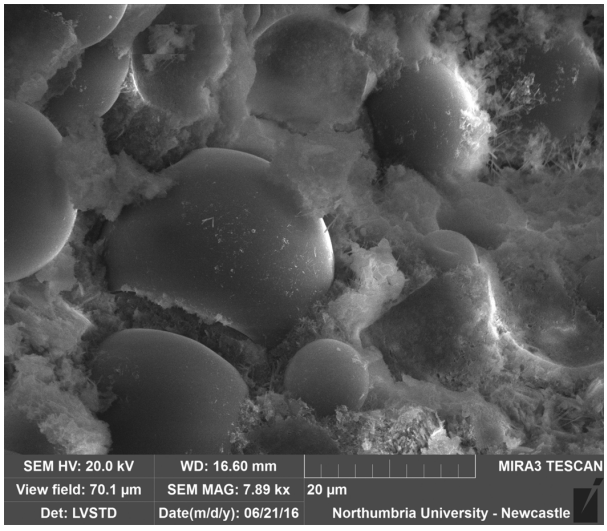

FIGURE 12. Mortar with PCM20% and SF30% (C40-SF30-PCM20)—broken particle ringed.

Figure 10 illustrates the standard mortar particles C100-SF0-PCM0 which exhibited good distribution, homogeneous and bonded particles. Figure 11 displays the mortar with PCM20% but without silica fume C100-SF0-PCM20, which indicates that most of the PCM particles are distributed, closed and bonded to the surrounding particle surfaces of cement. Figure 12 is the image of the mortar structure of the mix which contains PCM20% as Figure 10 but also contains SF30% (C70-SF30-PCM20) which shows the particles of both PCM and SF that seem to be about the same size and shape. The broken particles are evident on the failure surface in Figures 11 and 12. The reason for the particles breaking is because the PCM has low shear strength and stiffness and some of the PCM particles have failed during the test [27]. This explains, at the micro scale, why the compressive strength of the mortar is reduced when more PCM is combined. It can also be seen from the SEM images that the PCM particles are bonding well with the binder, which explains why the compressive strength of the mortar up to 20% PCM incorporation is acceptable.

3.2 Mechanical properties of PCM mortar

Compressive strength, flexural strength and direct tensile strength tests were performed on the mortar specimens in order to study the effect of PCM. These are of particular interest given the conflicting results from previous studies [28 and 29].

3.2.1 Compressive strength

Figure 13 displays the results of the relative compressive strengths at 28 days' age of all mixes. The control mix C100-SF0-PCM0 is used as the reference value.

FIGURE 13. Relative Compressive strength of mortar with PCM at 28 days' age.

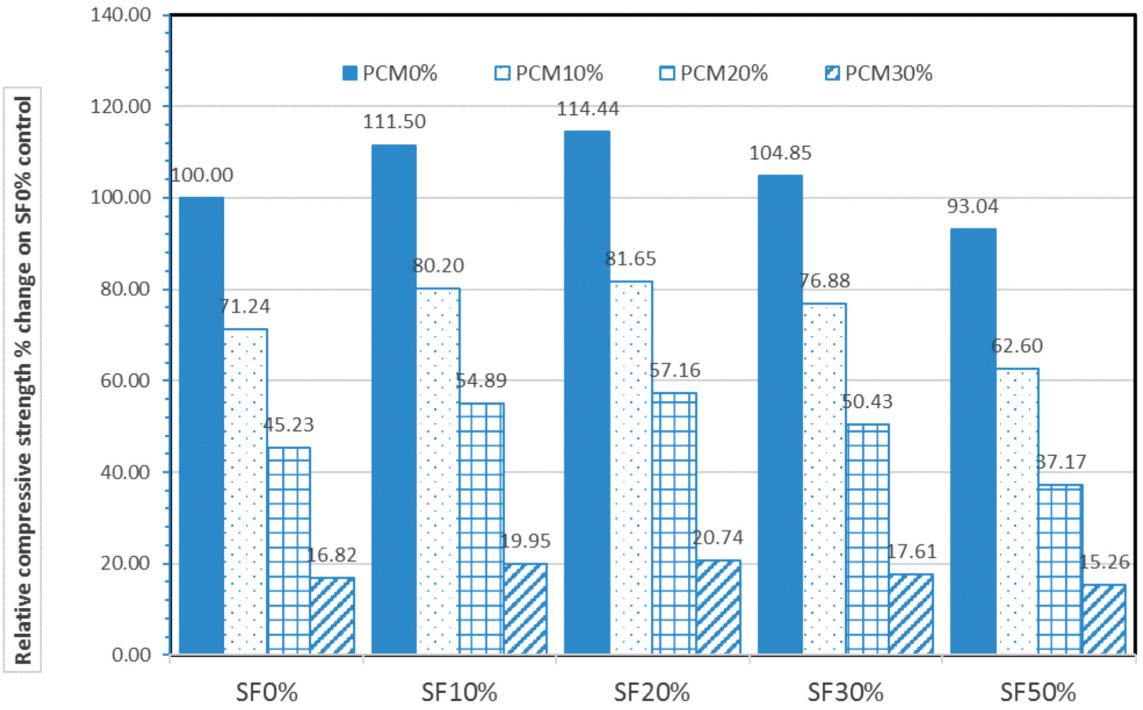

Figure 13 illustrates that specimens containing PCM display a reduced compressive strength. This was dependent upon the amount of PCM% added to the specimens. Specimens without silica fume recorded 71.24, 45.23 and 16.82% relative compressive strength for mortars containing 10, 20 and 30% PCM. All samples display improved compressive strength with the use of silica fume up to 30%, but the optimal silica fume was about 20%. The relative strengths increased and were recorded as 114.55, 81.65 and 57.16% respectively.

3.2.2 Flexural strength

Flexural strength for mortar specimens was carried out on a standard prism (40x40x160 mm). The results shown in Table 4 and Figure 14 indicates that the flexural strength declines with increasing PCM%. Silica fume was beneficial up to 10% but at more than this percentage the flexural strength is less than mixes without silica fume and reduces proportionately to the %SF added. The flexural strength for specimens without silica fume decreased from 3.50 to 1.66 MPa when increasing PCM% from 0 to 30%. Adding silica fume at the optimal rate of 10% improved the flexural strength performance to 3.60 and 1.75 MPa when PCM% was added by 0 and 30%.The percentage of flexural strength relative to compressive strength ranges between (12.3–38.6%) for specimens without silica fume and is directly proportional with the PCM%. When silica fume is added this variable ranges between (10.4–26.7%), (9.4–26.6%), (9.4–28.2%) and (11.6–36.6%) for specimens with SF% 10, 20, 30 and 50% respectively and again is directly proportion with the PCM%.

BS EN 1015-11:1999 was used to calculate the Flexural Strength of a mortar mix incorporating PCM with SF to within ±6% for SF10 through SF30 and ±16% for SF0 and SF50.

$$f_{\text{m-PCM}} = -0.00004 \cdot PCM\%^3 + 0.0014 \cdot PCM\%^2 - 0.0673 \cdot PCM\% + f_{\text{m}} \cdot (-0.004 \cdot SF\% + 1.0634)$$

Where: ($f_{\text{m-PCM}}$) is the Flexural Strength of the mortar incorporating PCM and SF (MPa); ($PCM\%$) is the percentage of PCM incorporated into the mortar; (f_{m}) is the Flexural Strength of standard mortar (MPa); and ($SF\%$) is the percentage of SF.

FIGURE 14. Flexural strength of mortar with PCM after 28 days.

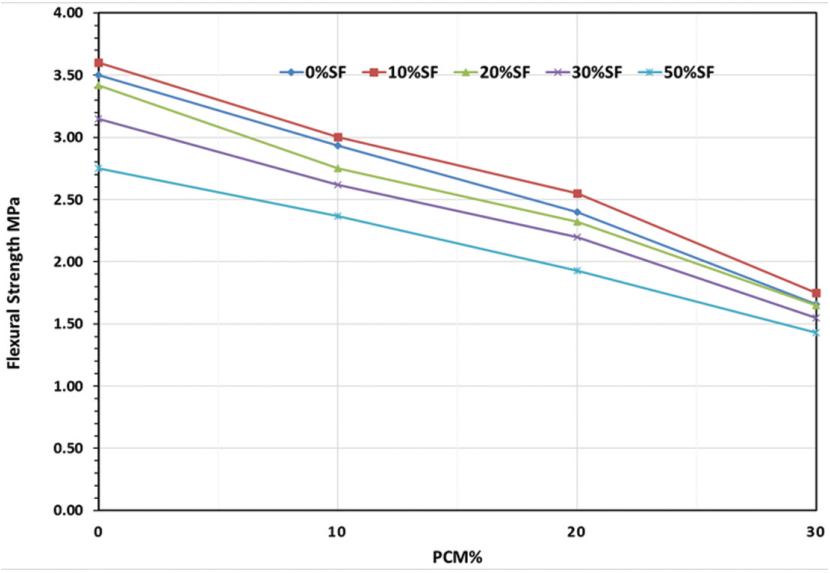

3.2.3 Indirect tensile strength

The indirect tensile strength of the specimens indicates one of the most important mechanical properties of the mortar. Cubes of dimensions 100x100x100 mm were prepared to measure the indirect tensile strength (Brazilian test). Table 4 and Figure 15 show the effect of PCM% on the indirect tensile strength where degradation of the tensile strength was noted for all specimens. For samples without silica fume (SF0%), the strength decreases from 2.65 to 0.75 MPa when increasing PCM up to 30%. Adding SF, up to 30%, did improve the tensile strength at all PCM concentrations with SF20% being optimal. At SF50% the tensile strength was less than the samples without any silica fume. With PCM0% the relative tensile strength to compressive strength improves slightly by adding silica fume (9.3, 7.8, 8.0, 8.3 and 10.2% for SF% 0, 10, 20, 30 and 50% respectively).

Equation [4] can be used to estimate the Tensile Strength of a mortar mix incorporating PCM with SF to within ±6% for SF0 through SF30.

$$T_{\text{m-PCM}} = 0.00002 \cdot PCM\%^3 - 0.0001 \cdot PCM\%^2 - 0.077 \cdot PCM\% + T_{\text{m}} \cdot (0.00000094 \cdot SF\%^4 - 0.000087 \cdot SF\%^3 + 0.00222 \cdot SF\%^2 - 0.0125 \cdot SF\% + 1.0)$$

Where; ($T_{\text{m-PCM}}$) is the Tensile Strength of the mortar incorporating PCM and SF (MPa); ($PCM\%$) is the percentage of PCM incorporated into the mortar; (T_{m}) is the Tensile Strength of standard mortar (MPa); ($SF\%$) is the percentage of SF.

FIGURE 15. Tensile strength of mortar with PCM after 28 days.

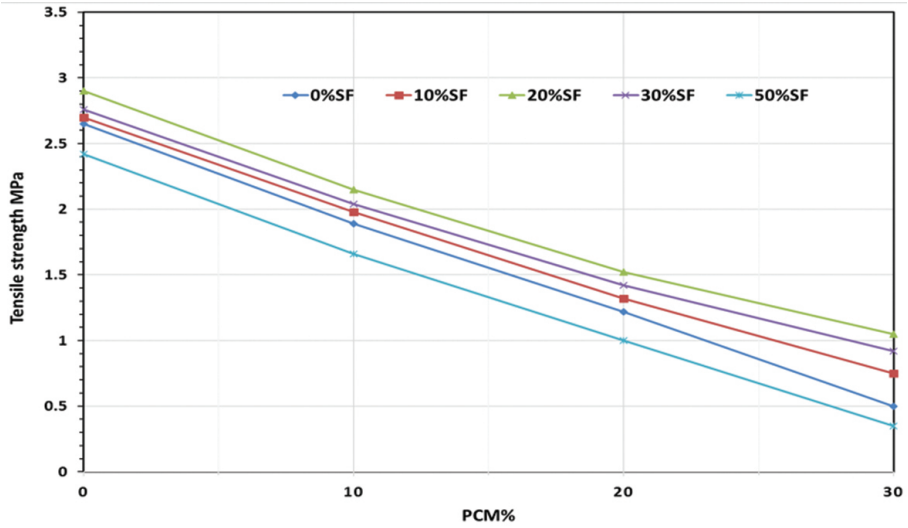

3.2.4 The role of Silica Fume

This study has demonstrated that Silica Fume improves the mechanical properties of mortar, including those incorporating PCM. The main mechanism for this improvement is summarised by Siddique and Chahal [5] as an increased bonding of the hydrated cement matrix with the sand thus increasing the strength. The extreme fineness of the SF also reduces voids within the mortar mix, reduces the air content and makes it a very reactive pozzolanic material. Appa Rao [6] provides additional detail regarding the pozzolanic reaction and explains that the SF reacts

with the calcium hydroxide created by the hydrolysis of Portland cement to produce additional calcium silicate and thus improve the performance of the mortar.

4. CONCLUSIONS

The effect of the incorporation of PCM and SF additives in mortars, when used as a plastered wall coating, was considered. The introduction of a phase change material (PCM) was assessed for mortars prepared with different percentages of silica fume and the PCM selected was composed of spherical aggregates with an average size of 17–20 μm. The mortars were evaluated for thermal efficiency using a thermal conductivity test. The mixtures with PCM have a lower thermal conductivity compared to the reference mortar, and the reduction is proportionate to the percentage of PCM added.

From this research, the following conclusions can be drawn:

1. Using phase change materials in mortar needs careful handling, dry mixing and water addition to maintain the consistency of the mix, it also consumes large volumes of water.
2. Compressive strength of the mortar, with phase change materials (10, 20 and 30%) and without silica fume was about 71, 45 and 17% compared to the control mix, however, mixes up to PCM20%, were within Class IV (> 6) according to BS EN 998-1:2016 and those with PCM30% were within Class III (3.5–7.5).
3. Adding up to 20% silica fume to the mortar with PCM increased the relative compressive strength, and all of the mixes were within Class IV. The addition of more than SF20% decreases the compressive strength.
4. The flexural strength of the mortar incorporating PCM decreased from 3.50 MPa to 1.65 MPa when adding PCM. However, the addition of SF10% improved the results and returned the optimal flexural strength.
5. The indirect tensile strength of the mortar decreased from 2.65 MPa to 0.50 MPa when adding PCM 0–30% however, adding SF20% was the best ratio for tensile strength enhancement of the mortar with PCM.
6. The optimal SF addition rate to improve the compressive and tensile strength of mortar with any PCM% is 20%, however, for optimal flexural strength, SF10% was ideal.
7. Bulk density and density of the PCM mortar decreased when related to the control specimen. The bulk density and density of the control specimen were 1807 and 1880 kg/m^3. These values were reduced to 1064 and 1110 kg/m^3 using PCM30% and SF50%.
8. Water absorption of PCM mortar increased from 9% for the control mix to 21% using PCM30%. This was without silica fume however; silica fume can reduce the water absorption from 21% to 16% if it is used at a rate of 50% (SF50%). The pore volume follows the same trend of the water absorption where the pore volume percentage increased with PCM and silica fume reduced the pore volume for all mixes with PCM.
9. The thermal conductivity of the PCM mortar and silica fume was 48% when compared to the thermal conductivity of the control mix which was 60% where no silica fume was used.

In conclusion, this research has shown that an optimal addition of PCM and silica fume can improve the physical and thermal performance of the mortar. This paper refines previous research work to define optimal performance and to enable a more environmentally friendly product that has energy saving potential to lower building CO_2 emissions.

5. REFERENCES

[1] Entrop, A., Brouwers, H., & Reinders, A. (2011). Experimental research on the use of micro-encapsulated phase change materials to store solar energy in concrete floors and to save energy in Dutch houses. Solar Energy, 85, 1007–1020.

[2] Jin, X., & Zhang, X. (2011). Thermal analysis of a double layer phase change material floor. Applied Thermal Engineering, 31, 1576–1581.

[3] Lin, K., Zhang, Y., Xu, X., Di, H., Yang, R., & Qin, P. (2005). Experimental study of under-floor electric heating system with shape-stabilized PCM plates. Energy and Buildings, 37, 215–220.

[4] Sharma, A., Tyagi, V., Chen, C., & Buddhi, D. (2009). Review on thermal energy storage with phase change materials and applications. Renewable and Sustainable Energy Reviews, 13, 318–345.

[5] Siddique R and Chahal N. (2011). "Use of silicon and ferrosilicon industry by-products (silica fume) in cement paste and mortar." *Resources, Conservation and Recycling*, Vol 55, Elsevier, pp. 739–744.

[6] Appa Rao G. (2003). "Investigations on the performance of silica fume-incorporated cement pastes and mortars." *Cement and Concrete Research*, Vol 33, Pergamon, pp. 1765–1770.

[7] Farid MM, Khudhair AM, Razack SAK, Al-Hallaj S. (2004). A review on phase change energy storage: materials and applications. *Energy Conversion & Management*, 45:1597–1615.

[8] Khudhair AM, Farid MM. (2004). A review on energy conservation in building applications with thermal storage by latent heat using phase change materials. *Energy Conversion & Management* 2004; 45:263–275.

[9] Kalnæsa SE, Jelle BP. (2015). Phase change materials and products for building applications: A state-of-the-art review and future research opportunities. *Energy and Buildings*, 94: 150–176.

[10] Aste N, Angelotti A, Buzzetti M. (2009). The influence of the external walls thermal inertia on the energy performance of well insulated buildings. *Energy and Buildings*, 41:1181–1187.

[11] Izquierdo-Barrientos MA, Belmonte JF, Rodríguez-Sánchez D, Molina AE, Almendros-Ibáñez JA. (2012). A numerical study of external building walls containing phase change materials (PCM). *Applied Thermal Engineering*; 47:73–85.

[12] Alawadhi EM. (2008). Thermal analysis of a building brick containing phase change material. *Energy and Buildings*; 40:351–357.

[13] Jin X, Medina MA, Zhang X. (2013). On the importance of the location of PCMs in building walls for enhanced thermal performance. *Applied Energy*; 106:72–78.

[14] Entrop AG, Brouwers HJH, Reinders AHME. (2011). Experimental research on the use of micro-encapsulated Phase Change Materials to store solar energy in concrete floors and to save energy in Dutch houses. *Solar energy*; 85:1007–1020.

[15] Kuznik F, Virgone J. (2009). Experimental assessment of a phase change material for wall building use. *Applied Energy*; 86:2038–2046.

[16] Cabeza LF, Castellon C, Nogues M, Medrano M, Leppers R, Zubillaga O. (2007). Use of microencapsulated PCM in concrete walls for energy savings. *Energy and Buildings*; 39:113–119.

[17] Shilei LV, Neng Z, Guohui F. (2006). Impact of phase change wall room on indoor thermal environment in winter. *Energy and buildings*; 38:18–24.

[18] Schossiga P, Henninga HM, Gschwandera S, Haussmann T. (2005). Micro-encapsulated phase-change materials integrated into construction materials. *Solar Energy Materials & Solar Cells*; 89:397–306.

[19] Athienitis AK, Liu C, Hawes D, Banu D, Feldman D. (1997). *Building and environment*; 32:405–410.

[20] BS EN 1015-11:1999 Methods of test for mortar and masonry. Determination of flexural and compressive strength of hardened mortar.

[21] BS EN 1015-1:1999 Methods of test for mortar and masonry. Determination of particle size distribution (by sieve analysis).

[22] BS EN 1015-2:1999 Methods of test for mortar and masonry. Bulk sampling of mortars and preparation of test mortars.

[23] BS EN 197-1:2011 Cement. Composition, specifications and conformity criteria for common cements.

[24] BS EN 480-5:2005 Admixtures for concrete, mortar and grout. Test methods. Determination of capillary absorption.

[25] Paula Kirton, Alan Richardson, Brian Agnew. (2013). Thermo-mechanical performance of concrete with alternative binder material, *Structural Survey*, Vol. 31 Iss 5 pp. 368–386.

[26] BS EN1015-10:1999 Methods of test for mortar for masonry. Determination of dry bulk density of hardened mortar.
[27] Gschwander S, Schossig P, Henning HM. (2005). Micro-encapsulated paraffin in phase change slurries. *Solar Energy Mater Solar Cells*; 89:307–15.
[28] S.S. Lucasa, V.M. Ferreiraa, J.L. Barroso de Aguiar. (2013). Latent heat storage in PCM containing mortars—Study of microstructural modifications. Energy and Buildings 66 724–731.
[29] Aguiar José1, Cunha S and Kheradmand M. (2015). Mortars with Phase Change Materials: Contribute to Sustainable, Key Engineering Materials Vol. 634 pp. 3–13.
BS EN 998-1:2016 Specification of mortar for masonry. Rendering and plastering mortar.
BS EN 1015-1:1999 Methods of test for mortar and masonry. Determination of particle size distribution (by sieve analysis).